American Mineralogist, Volume 75, pages 209–220, 1990

An experimental study of Na-K exchange between alunite and aqueous sulfate solutions

Roger E. Stoffregen
Department of Geological Sciences, Southern Methodist University, Dallas, Texas 75275, U.S.A.
Gary L. Cygan
U.S. Geological Survey, 959 National Center, Reston, Virginia 22092, U.S.A.

Abstract

We have investigated the alkali-exchange reaction $KAl_3(SO_4)_2(OH)_6 + Na^+ = NaAl_3(SO_4)_2(OH)_6 + K^+$ (Reaction 1) by reacting synthetic alunite and natroalunite with $0.5m$ $(Na,K)_2SO_4$ solutions at 250, 350, and 450 °C. Experimentally determined values of $\ln K_D$ (where K_D is defined as the molar ratio of Na to K in the solid over that in the solution) range from -0.63 to -1.32 at 450 °C and 1000 bars, from -0.79 to -2.40 at 350 °C and 500 bars, and from -1.46 to -4.13 at 250 °C and 500 bars. The value of $\ln K_D$ increases with increasing mole percent natroalunite at each temperature studied.

We have fit these results by using a subregular Margules model for alunite-natroalunite mixing. Individual-ion activity coefficients for aqueous Na^+ and K^+ at 250 °C and 500 bars were estimated using Pitzer's equations. At this temperature, γ_{Na^+} and γ_{K^+} are nearly equal and therefore cancel each other out in the expression for $\ln K$ for Reaction 1, and we have assumed this to be the case at 350 °C and 500 bars and 450 °C and 1000 bars as well. Least-squares fits of the data from two sets of runs on opposite sides of the presumed equilibrium boundary yield the following estimates of $\ln K_{(1)}$ and Margules parameters:

	$\ln K_{(1)}$	$W_{G,Na}$ (J·mol^{-1})	$W_{G,K}$ (J·mol^{-1})
450 °C, 1000 bars	−0.99(0.05)	1837(427)	3159(435)
350 °C, 500 bars	−1.73(0.26)	2867(1050)	4785(1229)
250 °C, 500 bars	−2.56(0.42)	4668(2091)	6443(4836)

We have used the 250 °C value of $\ln K_{(1)}$ together with an estimated heat capacity and entropy of natroalunite to obtain a $\Delta G^0_{f,natroalunite}$ at 25 °C and 1 bar of -4622.40 (± 1.91) kJ·mol^{-1}.

The experimental data demonstrate that alunite and natroalunite are completely miscible at 450 and 350 °C but do not rule out a solvus at 250 °C. Because of the large uncertainty in the mixing terms, particularly at 250 °C, we have not attempted to predict a consolute temperature. The degree of asymmetry in the solid solution, as measured by the ratio of $W_{G,K}$ to $W_{G,Na}$, is equal to 1.7 at both 450 and 350 °C. If this value remains constant with decreasing temperature, the consolute composition will be 64.5 mol% natroalunite.

Published data on the chemistry of natural alunites suggest that more sodic alunite is favored at higher temperature, a result that is consistent with our experimental results. However, there is little compositional evidence of immisciblity between alunite and natroalunite, even at surficial temperatures. This may reflect the paucity of information on fine-scale compositional variability in alunites, as well as the formation of metastable intermediate compositions in low-temperature environments.

Introduction

The mineral alunite [$KAl_3(SO_4)_2(OH)_6$] occurs in hydrothermal ore deposits (Meyer and Hemley, 1967; Hemley et al., 1969; Brimhall, 1980), hot springs (Raymahashay, 1969; Schoen et al., 1974; Aoki, 1983), sedimentary rocks (King, 1953; Goldbery, 1980), and low- to intermediate-grade aluminous metamorphic rocks (Wise, 1975; Schoch et al., 1985). Substitution of Na for K is common in alunites from each of these environments, and a complete range of Na contents up to greater than 95 mol% natroalunite (Moss, 1958; Chitale and Guven, 1987) has been reported. Numerous other species may also substitute for K, including NH_4^+ (Altaner et al., 1988), H_3O^+ (Ripmeester et al., 1986), and Ca^{2+} or Sr^{2+}, which are generally accompanied by substitution of an equimolar amount of PO_4^{3-} for SO_4^{2-} to maintain neutrality (Botinelly, 1976; Scott, 1987; Stoffregen and Alpers, 1987),

0003–004X/90/0102–0209$02.00

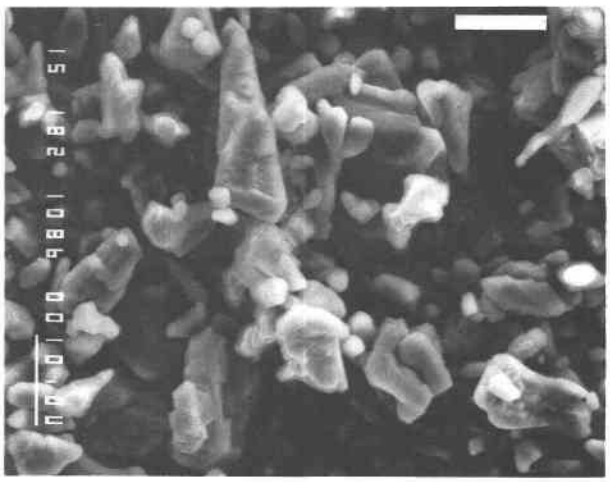

Fig. 1. SEM photo of synthetic natroalunite. Scale bar is 10 μm. This image was obtained with a JEOL-JXA733 scanning electron microscope using an accelerating voltage of 15 kV and a current of 100 nA.

but may also be compensated for by vacancies on the alkali site (Ossaka et al., 1982). However, these substitutions are in most cases insignificant compared to the amount of Na present.

In spite of the presence of Na in most natural alunite, little is known about the thermodynamic properties of natroalunite or of alunite-natroalunite solid solutions. Evidence of extensive miscibility between alunite and natroalunite, at least above 100 °C, is provided by the mineral-synthesis experiments of Parker (1962) and by compositional data on natural alunite reported in the literature. However, these data are inadequate to develop a mixing model for alunite-natroalunite. In this paper, we discuss a series of exchange experiments we have conducted with alunite and natroalunite and $0.5m$ $(Na,K)_2SO_4$ aqueous solutions at temperatures of 250 to 450 °C and pressures of 500 and 1000 bars. We have used the experimental data to obtain equilibrium constants for the alkali-exchange reaction and to compute subregular Margules terms describing alunite-natroalunite mixing at each temperature studied.

Experimental methods

Experiments were performed with synthetic alunite-natroalunite solid solutions ranging in composition from $X_{Na} = 0$ to $X_{Na} = 1.0$. End-member alunite and natroalunite were prepared using a modified version of the technique described by Parker (1962). Starting solutions containing 255 mL of distilled deionized H_2O, 16 g of $Al_2(SO_4)_3 \cdot 18H_2O$, and 4 g of K_2SO_4 or Na_2SO_4 were prepared using reagent-grade chemicals. These solutions were heated for 4 to 6 d at 150 °C and vapor-saturation pressure, producing well-crystallized alunite grains 2 to 20 μm in size (Fig. 1). However, this material was low in alkalis by 10 to 20 mol% relative to stoichiometric alunite and natroalunite. This alkali deficiency has been observed in most alunite-synthesis experiments and has been attributed to the presence of H_3O^+ on the alkali site (Parker, 1962; Fielding, 1980; Ripmeester et al., 1986). We found that this deficiency could be eliminated by heating the synthetic alunites in $1.0m$ Na_2SO_4 or $0.7m$ K_2SO_4 for 7 to 10 d at 250 °C. This heating step is presumed to cause exchange of Na or K for hydronium.

All charges were sealed in cleaned and annealed Au capsules 4 to 8 cm in length and 5 to 7 mm in diameter. These were run in standard large-capacity cold-seal hydrothermal vessels having an inner diameter of 0.6 to 1.5 cm. Temperatures were measured by chromel-alumel thermocouples calibrated against a Pt-Rh standard and are believed accurate to ±2 °C. Water served as the pressure medium. Pressures were measured with a Heise gauge and are believed accurate to ±5% of the measured value.

The approximate amount of fluid required to fill each capsule at its run conditions was determined by using the volumetric properties of water. These amounts generally ranged from 0.30–0.35 cm^3 at 450 °C to 0.50–0.80 cm^3 at 250 °C. The 250 and 350 °C experiments were run at 500 bars, and the 450 °C experiments were run at 1000 bars. Higher pressure was used at 450 °C to compensate for the large increase in the molar volume of water between 350 and 450 °C at 500 bars (Helgeson and Kirkham, 1974). The increased pressure allowed for larger starting fluid volumes and thus facilitated collection and analysis of the run-product solutions. Starting fluid/alunite mass ratios ranged from 1 to 30 and were generally between 2 and 10.

Run times ranged from 1–4 weeks at 450 °C to 3–4 months at 250 °C. Where adequate reversals could not be obtained over these run times using pure alunite or natroalunite starting material, experiments were repeated using washed and re-ground alunites of intermediate composition produced in previous experiments. Runs were quenched in ice water or in compressed air, with quench times to 100 °C not exceeding 5 min. Run-product alunites were digested in concentrated HF, and these digestates, along with the run-product solutions and blanks, were analyzed for Na and K on a Perkin and Elmer[1] atomic absorption spectrophotometer using standard techniques for suppression of ionization. Precision of these analyses was generally from 2% to 3%. Sulfate was determined on some of the run-product solutions using a Dionex model 2012-I ion chromatograph. Precision of these analyses was approximately ±7%.

Results

Alkali exchange between alunite and aqueous solution may be represented by the reaction

$$KAl_3(SO_4)_2(OH)_6 + Na^+ = NaAl_3(SO_4)_2(OH)_6 + K^+. \quad (1)$$

Defining the distribution coefficient K_D for this exchange

[1] Any use of trade, product, or firm names in this publication is for descriptive purposes only and does not imply endorsement by the U.S. Government.

as $(X_{Na}/X_K)/(m_{Na}/m_K)$, where X indicates the mole fraction in the solid and m the molality in the aqueous solution, we can write at equilibrium

$$-RT \ln K_D = \Delta G^0_{r,P,T} + (dG_{xs,alun}/dX_{Na}) - (dG_{xs,soln}/dN_{Na}). \quad (2)$$

$\Delta G^0_{r,P,T}$ in this equation is the standard-state Gibbs free-energy change for Reaction 1 at a given pressure and temperature, the G_{xs} terms are the excess Gibbs free energy of mixing in the solid and in the aqueous solution, X_{Na} is the mole fraction of Na in the solid and N_{Na} is the molar Na/(Na + K) ratio in the aqueous solution. Computed values of ln K_D are tabulated in Table 1 along with other data on each run. The experimental results are also illustrated in Figure 2.

Experimentally determined values of K_D can be used to compute the standard-state Gibbs free energy of Reaction 1 at P and T and the excess Gibbs free energy of the solid in Equation 2. In order to make these calculations, it is first necessary to consider the term related to mixing in the aqueous phase. In the following treatment, we have assumed that this term is negligible and can be ignored. This assumption can be justified at 250 °C by use of Pitzer's equations (e.g., Pabalan and Pitzer, 1987) to compute Na^+ and K^+ individual-ion activity coefficients, as discussed in Appendix 1. Similar calculations cannot be made for our higher-temperature experiments because the necessary Pitzer coefficients at these temperatures are not now available. The validity of neglecting these activity coefficients in the 350 and 450 °C experiments is discussed below.

Measured values of ln K_D are plotted against X_{Na} in Figure 3. We have fit these data by using a subregular Margules model (e.g., Thompson and Waldbaum, 1968), which assumes that the excess free energy of the solid can be expressed as $G_{xs} = X_K X_{Na}(W_{Na}X_K + W_K X_{Na})$. This model is necessary to describe the nonlinear variation in ln K_D with alunite composition that is evident in Figure 3. Although some authors (e.g., Powell, 1987) have emphasized the theoretical inconsistencies of the Margules approach, it nonetheless provides a useful mathematical representation of our experimental data. Moreover, the experimental constraints we have obtained are inadequate to discriminate between a Margules model and other approaches such as the quasi-chemical mixing model (Green, 1970) or quadratic formalism (Powell, 1987). Work currently in progress on volumes of mixing for alunite-natroalunite (Stoffregen and Alpers, in preparation) may provide additional constraints on the functional form of this mixing term.

Substituting the subregular Margules expression for $G_{xs,alun}$ into Equation 2, setting $dG_{xs,soln}/dN_{Na}$ equal to zero (which is equivalent to setting the activity-coefficient ratio $\gamma_{Na^+}/\gamma_{K^+}$ equal to unity) and dividing through by $-RT$ yields

$$\ln K_D = \ln K_{(1)} + (W_{G,Na}/RT)(-3X^2_{Na} + 4X_{Na} - 1) + (W_{G,K}/RT)(3X^2_{Na} - 2X_{Na}). \quad (3)$$

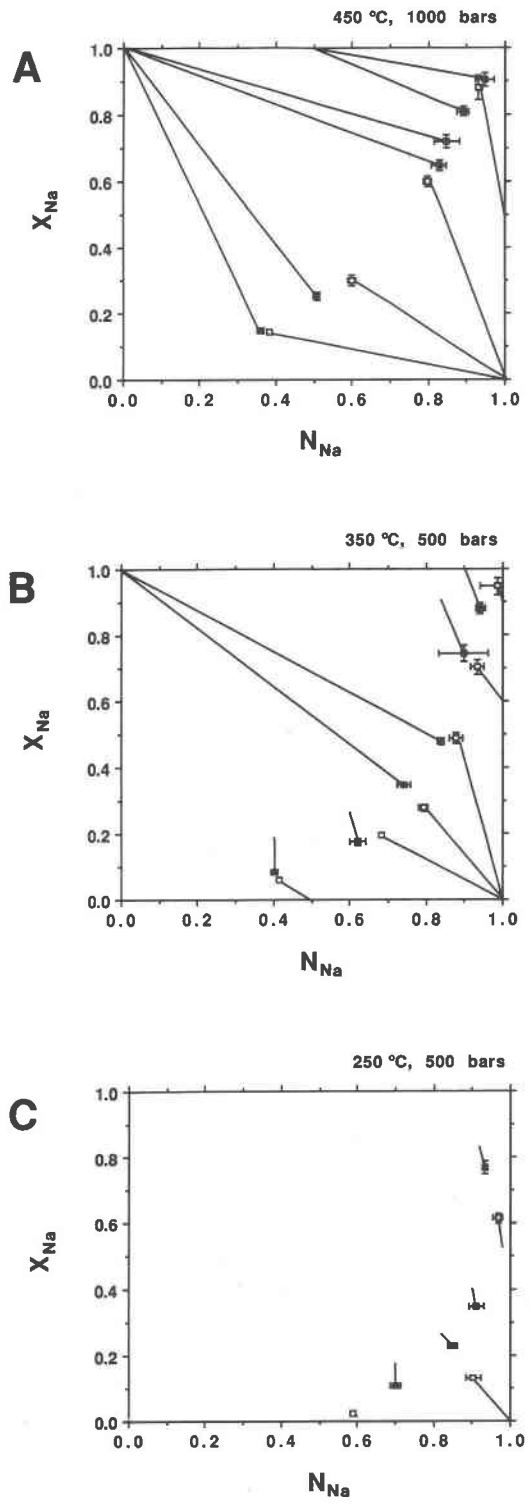

Fig. 2. Experimental data on alunite and aqueous solution compositions at (A) 450 °C and 1000 bars, (B) 350 °C and 500 bars, and (C) 250 °C and 500 bars. Open symbols indicate runs in which X_{Na} increased, and filled symbols, runs in which X_{Na} decreased. Error bars represent analytical error. Lines connect starting and final solution and alunite compositions.

TABLE 1. Composition of starting and final alunite and aqueous solution

Run	Duration (d)	Starting X_{Na}	Starting N_{Na}	Final X_{Na}	σ	Final N_{Na}	σ	ln K_D	σ	Final m_{SO_4}
T = 450 °C, P = 1000 bars										
68	14	0.00	1.00	0.298	0.0159	0.600	0.0097	−1.26	0.056	1.19
69	14	1.00	0.50	0.811	0.0132	0.891	0.0160	−0.64	0.056	
70	7	1.00	0.00	0.598	0.0160	0.804	0.0113	−0.98	0.031	
75	7	1.00	0.00	0.146	0.0058	0.361	0.0090	−1.18	0.047	
80*	32	0.00	1.00	0.649	0.0147	0.828	0.0187	−0.96	0.032	1.13
81*	31	0.53	1.00	0.880	0.0360	0.932	0.0085	−0.63	0.054	1.21
82	30	0.00	0.50	0.142	0.0044	0.383	0.0040	−1.32	0.034	1.21
84	30	1.00	0.00	0.252	0.0106	0.508	0.0099	−1.12	0.055	
98*	21	1.00	0.00	0.720	0.0204	0.848	0.0325	−0.77	0.043	
105	19	1.00	0.50	0.904	0.0217	0.948	0.0240	−0.65	0.037	
T = 350 °C, P = 500 bars										
4	16	0.00	1.00	0.195	0.0037	0.684	0.0049	−2.19	0.028	
6	28	1.00	0.00	0.347	0.0060	0.741	0.0175	−1.68	0.049	
8	28	0.00	1.00	0.278	0.0087	0.793	0.0117	−2.30	0.035	
46	115	1.00	0.00	0.478	0.0108	0.839	0.0092	−1.73	0.024	
48	115	0.00	0.50	0.060	0.0018	0.413	0.0061	−2.40	0.034	
49	115	0.00	1.00	0.488	0.0177	0.877	0.0171	−2.01	0.040	
77	51	1.00	0.90	0.880	0.0162	0.942	0.0129	−0.79	0.033	0.82
78	35	0.18	0.40	0.084	0.0012	0.402	0.0082	−1.99	0.036	0.74
79	44	0.26	0.60	0.175	0.0100	0.621	0.0213	−2.05	0.070	0.79
90	43	0.60	1.00	0.703	0.0211	0.934	0.0165	−1.79	0.038	0.77
107	28	0.90	1.00	0.947	0.0264	0.986	0.0451	−1.38	0.052	0.72
113	28	0.90	0.84	0.744	0.0249	0.898	0.0652	−1.11	0.069	
T = 250 °C, P = 500 bars										
13	92	0.00	1.00	0.132	0.0044	0.904	0.0187	−4.13	0.043	
42	120	0.40	0.90	0.346	0.0066	0.911	0.0191	−2.96	0.025	
43	120	0.02	0.60	0.025	0.0009	0.590	0.0049	−4.02	0.037	
85	91	0.18	0.70	0.107	0.0037	0.701	0.0138	−2.96	0.041	0.51
86	90	0.26	0.82	0.228	0.0044	0.850	0.0133	−2.95	0.028	0.52
87	91	0.83	0.92	0.768	0.0202	0.934	0.0081	−1.46	0.034	0.56
88	90	0.53	0.98	0.615	0.0147	0.967	0.0118	−2.91	0.036	

Note: The molality of Na_2SO_4 + K_2SO_4 in all starting solutions was 0.5.
* Denotes runs with 0.3m H_2SO_4 in the starting solution.

Using this expression, we have fit the experimental values of ln K_D and X_{Na} to obtain ln $K_{(1)}$, $W_{G,Na}$, and $W_{G,K}$ at each temperature. The lack of complete reversibility in the experiments, even at 450 °C, necessarily limits the precision of these estimates of ln $K_{(1)}$, $W_{G,Na}$, and $W_{G,K}$.

In order to obtain realistic uncertainties for the ln $K_{(1)}$ values we performed two least-squares fits at each temperature, one for those runs that approached equilibrium from the natroalunite side and another for the remaining runs. Data points were weighted by the reciprocal of the error associated with ln K_D. This approach provided a maximum and minimum ln $K_{(1)}$ value at each temperature, and the resulting best estimate for ln $K_{(1)}$ was taken as the average of these two values (cf. Zen, 1972). These values are tabulated in Table 2A.

Estimates of $W_{G,K}$ and $W_{G,Na}$ were obtained at 450 and 350 °C by using least squares fits of the experimental data, again weighted by the reciprocal of the error in ln K_D. These estimates are tabulated in Table 2B, along with 1σ of error associated with the fit. These errors do not provide a true measure of the uncertainty in the W terms because the data points are not normally distributed about the equilibrium value (cf. Zen, 1972). The true error of these estimates is a larger, but indeterminant, value. Although it is difficult to quantify the uncertainties associated with these fit parameters, we think that this approach provides the best available estimates for the W terms. Curves generated by using the computed W values are compared with the experimental data in Figure 3.

The experimental data at 250 °C were also fit by using this method to obtain Margules values (Table 2B). The large uncertainties at this temperature reflect the relatively poor experimental reversals and the lack of experimental data for X_{Na} above 0.768. These large errors limit the utility of these terms in describing the mixing of alunite-natroalunite at 250 °C.

Incongruent alunite dissolution

Alkali exchange between alunite and solution was accompanied by incongruent alunite dissolution at each temperature studied. At 250 and 350 °C, formation of boehmite was observed in run products by the reaction

$$(K,Na)Al_3(SO_4)_2(OH)_6 = \underset{\text{(boehmite)}}{3AlO(OH)} + (K,Na)^+ + 3H^+ + 2SO_4^{2-}. \quad (4)$$

At 450°C, corundum was formed by the reaction

$$2(K,Na)Al_3(SO_4)_2(OH)_6 = \underset{\text{(corundum)}}{3Al_2O_3} + 2(K,Na)^+ + 4SO_4^{2-} + 6H^+ + 3H_2O. \quad (5)$$

TABLE 2A. Experimentally determined ln K values for Reaction 1

	Maximum*	Minimum*	Average†
450 °C, 1000 bars	−0.96	−1.03	−0.99
	(0.02)	(0.001)	(0.05)
350 °C, 500 bars	−1.51	−1.95	−1.73
	(0.04)	(0.04)	(0.26)
250 °C, 500 bars	−2.17	−2.96‡	−2.56
	(0.05)	—	(0.42)

* Error given in parentheses is 1σ associated with the least-squares fit.
† The error in parentheses is half the difference between the maximum value $+\sigma$ and the minimum value $-\sigma$.
‡ No error could be computed for this fit because only three points were used to determine the three fit parameters.

TABLE 2B. Experimentally determined Margules parameters (in J·mol^{-1})

	$W_{G,Na}$	$W_{G,K}$
450 °C, 1000 bars	1837	3159
	(427)	(435)
350 °C, 500 bars	2867	4785
	(1050)	(1229)
250 °C, 500 bars	4668	6443
	(2091)	(4836)

Note: Values in parentheses give 1σ of error associated with the fit.

Both reactions lead to an increase in the molality of $(Na,K)_2SO_4$ during the run and to the formation of sulfuric acid.

Incongruent alunite dissolution becomes more significant at higher temperatures. At 250 °C, boehmite was observed in XRD patterns of the run products only in runs with high fluid/alunite ratios. This is consistent with sulfate concentrations measured in three of the 250 °C run-product solutions [which are only slightly elevated above the starting value of 0.5m (Table 1)] and suggests that the amount of alunite dissolution by Reaction 4 was minimal at this temperature. At 350 °C, boehmite formed in all runs, and sulfate concentrations were in the range of 0.72–0.82m (Table 1) in the run-product solutions. Incongruent alunite dissolution was even more pronounced at 450 °C, at which temperature alunite was totally converted to corundum at starting fluid/alunite ratios greater than 10. The increase in alunite dissolution at 450 °C is also indicated by elevated sulfate concentrations in run-product solutions of 1.13–1.21m (Table 1).

In order to suppress Reaction 5 and prevent conversion of all the starting alunite to corundum, 0.3m H_2SO_4 was added to some of the 450 °C runs (indicated with an asterisk in Table 1) along with 0.5m $(Na,K)_2SO_4$. This reduced the amount of corundum formation although it did not eliminate it entirely. The final solution composition in these runs, as in those without H_2SO_4 in the initial solution, was therefore controlled by the alunite-corundum equilibrium represented by Reaction 5.

Gibbs free energy of mixing in the aqueous phase

The H_2SO_4 generated by Reactions 4 and 5 may affect K_D by changing the behavior of the $dG_{xs,soln}/dN_{Na}$ term in Equation 2. The excess term for the aqueous phase may also be expressed as $-RT(\ln \gamma_{Na^+} - \ln \gamma_{K^+})$, where γ represents the individual-ion activity coefficient. This difference may be a function of aqueous-solution composition as well as temperature and pressure.

Although the quantity $\ln \gamma_{Na^+} - \ln \gamma_{K^+}$ cannot be computed for the reactions taking place at high temperature, some insight into the effect of changes in sulfuric acid

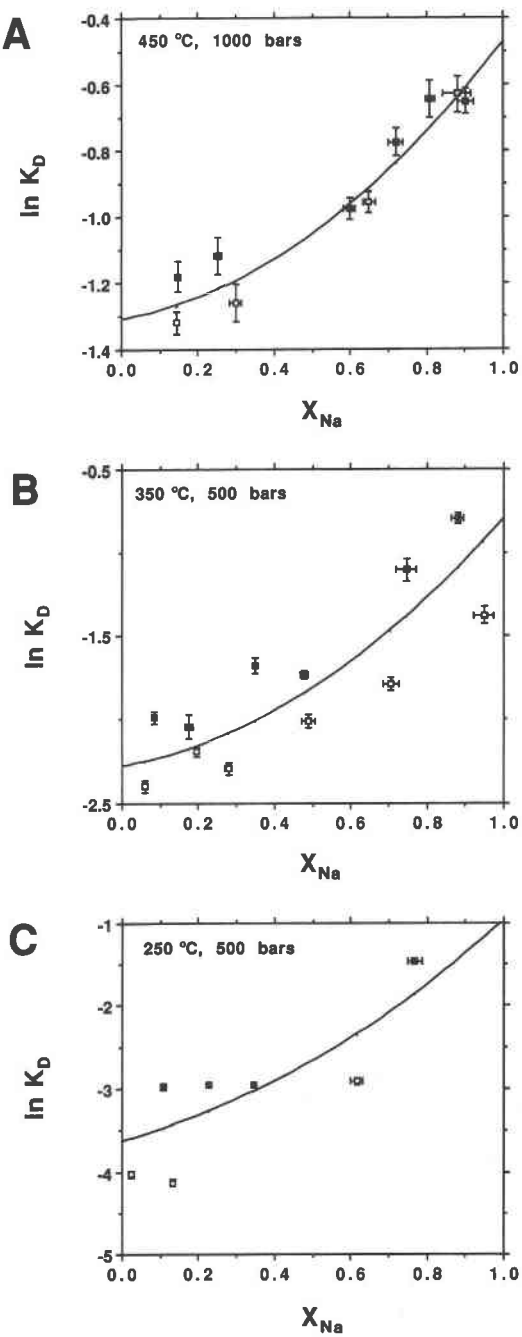

Fig. 3. Plots of ln K_D versus X_{Na} at (**A**) 450 °C, (**B**) 350 °C, and (**C**) 250 °C. Symbols and error bars are as in Fig. 2. Also shown are curves calculated from the subregular Margules parameters listed in Table 2B.

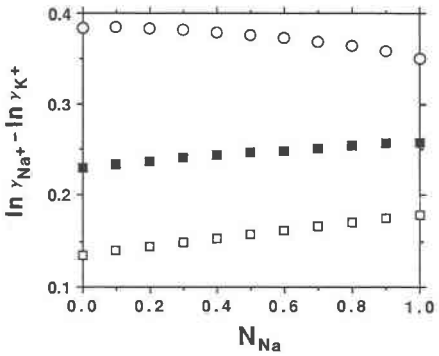

Fig. 4. Effect of N_{Na} on the calculated quantity ($\ln \gamma_{Na^+} - \ln \gamma_{K^+}$) for $0.5m$ $(Na,K)_2SO_4$ solutions containing $0.5m$ (open squares), $1.0m$ (solid squares), and $2.0m$ (open circles) H_2SO_4. Values are computed for a solution at 25 °C using Pitzer coefficients from Harvie et al. (1984) and a dissociation constant for HSO_4^- of 0.0105 (from Pitzer et al., 1977).

concentration on this term can be obtained by considering the system K_2SO_4-Na_2SO_4-H_2SO_4-H_2O at 25 °C. Using fit parameters for Pitzer's equations from Harvie et al. (1984), we can compute γ_{Na^+} and γ_{K^+} for a $0.5m$ $(Na,K)_2SO_4$ solution at this temperature for a range of H_2SO_4 concentrations. Calculated values of $\ln \gamma_{Na^+} - \ln \gamma_{K^+}$ as a function of N_{Na} are shown for $0.5m$, $1.0m$, and $2.0m$ H_2SO_4 solutions in Figure 4. The plot illustrates that this quantity is not strongly dependent on N_{Na} but becomes significantly more positive with increasing molality of H_2SO_4. This behavior indicates that at 25 °C K^+ interacts more strongly with HSO_4^- than does Na^+ and implies that increases in the molality of sulfuric acid in the solution should favor the formation of more sodic alunite at constant N_{Na}.

Figure 4 suggests that in sulfuric acid–bearing solutions, it may be more reasonable to assume that the excess Gibbs free energy of the aqueous solution at a given temperature and pressure is constant rather than zero (provided molality of H_2SO_4 remains relatively constant). If the excess Gibbs free energy of the aqueous solution is assumed constant, then each measured K_D value at a given temperature would need to be corrected by addition of a constant equal to $-(\ln \gamma_{Na^+} - \ln \gamma_{K^+})$ prior to fitting the data for $\ln K_{(1)}$. Figure 4 suggests that this correction would lead to more negative values of $\ln K_{(1)}$ than those obtained using uncorrected K_D values from our 350 and 450 °C experiments. However, this term would not affect the amount of change in K_D as a function of solid composition, and would therefore not change the mixing parameters obtained from fitting the uncorrected K_D values.

In order to examine the effect of changes in sulfuric acid concentration on K_D, we conducted a second set of experiments at 450 °C and 1000 bars. The starting solutions in these runs contained $0.5m$ $(Na,K)_2SO_4$ and $1.0m$ H_2SO_4 (Table 3). As expected, the initially high sulfuric acid concentration eliminated the formation of corundum by Reaction 5, but a new phase not observed in any

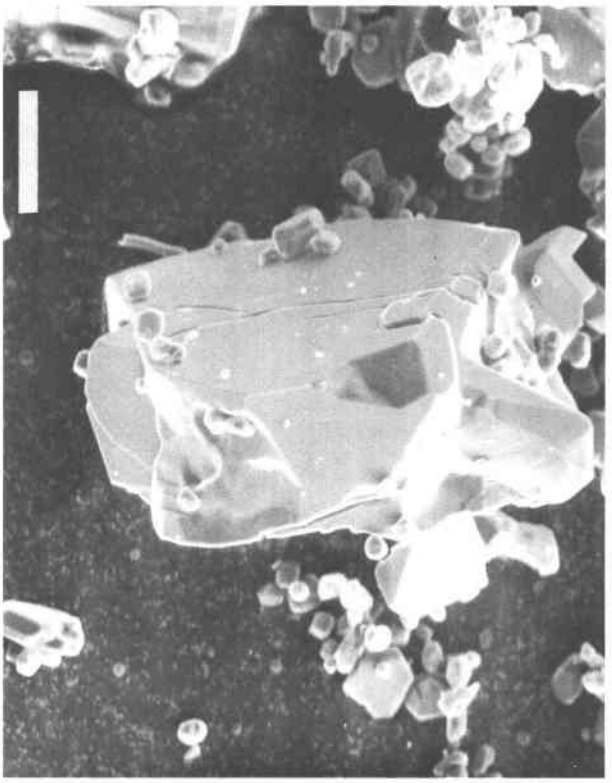

Fig. 5. SEM photo of the aluminum sulfate phase (large grain) produced in 450 °C runs with $1.0m$ H_2SO_4 in addition to $0.5m$ $(Na,K)_2SO_4$ in the starting solution. The image was obtained with a JEOL JXA-733 scanning electron microscope using an accelerating voltage of 15 kV and a current of 100 nA. Scale bar is 40 μm.

of the previous runs was produced. This phase was recognized on diffractograms of the run-product solids, but could not be matched with any entry in the JCPDS card file although it shows some similarity with an aluminum sulfate phase described by Davey et al. (1963). Scanning-electron-microscope study of these run products indicated that the unknown phase is relatively coarse grained (Fig. 5) and contained Al and S but no alkalis.

The occurrence of this aluminum sulfate phase indicates that in these runs, the aqueous solution was again buffered by partial alunite dissolution. In this case the alunite dissolution consumed rather than produced aqueous sulfate, as indicated by the decrease in sulfate molality in the run-product solutions (Table 3).

Although sulfate decreased during these runs, its final concentration was still greater than that observed for the earlier series of 450 °C runs buffered by alunite-corundum equilibrium. This change in aqueous-solution composition appears to have displaced the measured values of $\ln K_D$ to slightly higher values, as illustrated in Figure 6. This observation is consistent with Figure 4, which suggests that higher sulfuric acid concentrations should increase the $\ln \gamma_{Na^+} - \ln \gamma_{K^+}$ term and also increase mea-

sured values of K_D. However, the curvature of ln K_D with alunite composition appears similar to that defined by the previous experiments (Fig. 3A), with the exception of the most Na-rich alunite. The significance of this point is not clear.

These results suggest that our computed ln $K_{(1)}$ values at 350 and 450 °C may be too large. However, they are in general agreement with our previous assumption that the variation in ln K_D with alunite composition is produced largely, if not exclusively, by the mixing properties of alunite-natroalunite and not by those of the aqueous phase.

Discussion

We feel that the experimental data provide two important qualitative results on the mixing relations of alunite and natroalunite. First, they suggest that both $W_{G,Na}$ and $W_{G,K}$ for alunite-natroalunite mixing increase with decreasing temperature. This behavior is typical of many solid solutions (Powell, 1974) and favors the formation of a solvus between alunite and natroalunite as temperature decreases. This solvus cannot occur at or above 350 °C, where our experimental results demonstrate complete miscibility. However, these results do not preclude a miscibility gap at 250 °C. Without more precise knowledge of the variation in W_G values with temperature, it is impossible to make a meaningful estimate of the consolute temperature beyond these broad constraints.

The estimated Margules terms also suggest that the degree of asymmetry in the alunite-natroalunite solid solution, as measured by the ratio of $W_{G,K}$ to $W_{G,Na}$, remains relatively constant with decreasing temperature. Our computed $W_{G,K}/W_{G,Na}$ ratio varies only slightly from 1.72 to 1.67 between 450 and 350 °C. If this ratio is assumed to remain constant at 1.7 with decreasing temperature, the method of Guggenheim (1952) can be used to predict a consolute composition of 64.5 mol% natroalunite. This value, along with the apparent increase in W terms with decreasing temperature, suggests that an asymmetric solvus is present in the alunite-natroalunite system.

The asymmetry indicated by the Margules mixing terms implies that it is easier to substitute Na^+ for K^+ in alunite than to substitute K^+ for Na^+ in natroalunite. This probably reflects the greater size of the K^+ ion. When in 12-fold coordination, as occurs on the alkali site in alunite, K^+ has an ionic radius roughly 20% greater than that of

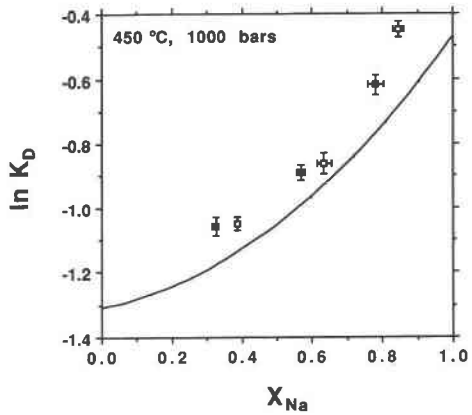

Fig. 6. Plot of ln K_D versus alunite composition for runs that included 1.0m H_2SO_4 in the starting solution. Also shown is the curve from Fig. 3A generated from the best-fit values of ln $K_{(1)}$, $W_{G,K}$, and $W_{G,Na}$ from Tables 2A and 2B.

Na (Shannon, 1976). The larger size of the K^+ ion is also reflected in the molar volumes of the two end-members, which increase from 141.15 cm³/mol for natroalunite to 146.80 cm³/mol for alunite (Parker, 1962). As noted by Davies and Navrotsky (1983), volume differences between end-members are more useful for predicting the magnitude of excess mixing terms than are differences between the radii of the ions involved in the substitution.

The mixing behavior of alunite-natroalunite can be compared with other Na-K binary solid solutions, including muscovite-paragonite, alkali feldspar, and alkali halides. Figure 7 compares Margules parameters for alunite-natroalunite with values for muscovite-paragonite at 420 °C and 1000 bars from Pascal and Roux (1985), for alkali feldspar at 500 °C and 1000 bars from Thompson and Waldbaum (1969), and for alkali iodides, bromides, and chlorides. The Margules terms for the alkali halides are shown only at the consolute temperature for each system and were computed by using data on their consolute temperatures and compositions from Chanh (1964). Although other models are available to describe mixing in some of these systems (e.g., Powell, 1974), we have used only the subregular Margules terms to facilitate comparison with our alunite data.

Figure 7 illustrates that $W_{G,K}$ is greater than $W_{G,Na}$ in each of these systems. Thus the expectation that the

Table 3. Composition of starting and final alunite and aqueous solution

Run	Duration (d)	Starting X_{Na}	Starting N_{Na}	Final X_{Na}	σ	Final N_{Na}	σ	ln K_D	σ	Final m_{SO_4}
119	28	1.00	0.00	0.325	0.0089	0.581	0.0068	−1.05	0.029	
121	28	0.00	1.00	0.633	0.0217	0.802	0.0031	−0.86	0.034	1.38
123	32	0.00	0.50	0.780	0.0232	0.867	0.0084	−0.62	0.031	1.21
124	32	0.53	1.00	0.844	0.0157	0.894	0.0110	−0.45	0.024	1.33
125	32	1.00	0.00	0.567	0.0120	0.761	0.0041	−0.89	0.023	1.33
126	32	0.00	1.00	0.385	0.0071	0.641	0.0039	−1.05	0.021	1.34

Note: For these runs, the starting solution contained 0.5m $(K,Na)_2SO_4$ and 1.0m H_2SO_4. These experiments were all run at 450 °C and 1000 bars.

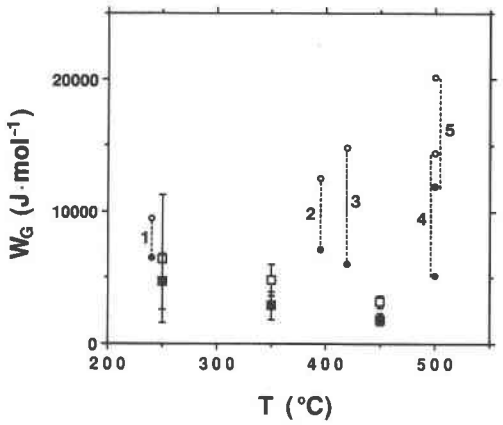

Fig. 7. Comparison of Margules values obtained in this study for alunite with selected values from other Na-K solid solutions. Alunite $W_{G,Na}$ with $W_{G,K}$ values are shown in solid and open squares, respectively. $W_{G,Na}$ and $W_{G,K}$ for other systems are shown with solid and open circles and are connected with dashed lines. The systems shown are alkali iodides (1), bromides (2), and chlorides (4) (Chanh, 1964); muscovite-paragonite (3) (Pascal and Roux, 1985); and alkali feldspar (5) (Thompson and Waldbaum, 1969).

smaller Na^+ ion should substitute more readily for K^+ than vice versa appears valid for a variety of mineral structures and compositions. It is also noteworthy that the consolute composition for the alkali halides (Chanh, 1964), alkali feldspar (Thompson and Waldbaum, 1969), muscovite-paragonite (Chatterjee and Flux, 1986), and the predicted value for alunite all are within the range of $X_{Na} = 0.62$ to 0.75. There are, however, some systems that do not conform to this pattern of asymmetric mixing between Na and K end-members. The system Na_2SO_4-K_2SO_4, for example, appears to have a nearly symmetric solvus, on the basis of the data of Perrier and Bellanca (1940). This implies that the Margules terms for Na and K are roughly equal and that the system can be modeled as a regular solution with only one mixing term. Ion-exchange data from Ames (1964) suggests that many Na- and K-bearing zeolite minerals are completely miscible at 25 °C. This complete miscibility at low temperature implies that the energetics of Na-K mixing in zeolites are substantially different from those of Na-K mixing in alunite and in the silicate minerals described above.

Thermodynamic data for natroalunite

The ln K for Reaction 1 can be used to calculate $G^0_{natroalunite}$ at the experimental temperature and pressure conditions. We have computed a value for $G^0_{natroalunite}$ at 250 °C and 500 bars of -4719.00 (± 1.91) kJ·mol^{-1} by using data from Helgeson et al. (1978) on the Gibbs free energy for alunite, Na^+, and K^+. Although the uncertainty in ln $K_{(1)}$ is larger at 250 °C than at higher temperatures, the 250 °C value is considered more reliable because it was obtained without making any assumptions about the aqueous activity terms (beyond those made in using Pitzer's equations at this temperature, as discussed in App. 1).

Table 4. Estimated thermodynamic properties of natroalunite at 25 °C and 1 bar

	ΔG_f	-4622.40 kJ·mol^{-1} ± 1.91 kJ·mol^{-1}*
	ΔH_f	-5131.97 kJ·mol^{-1}
	S†	321.08 J·K^{-1}·mol^{-1}
	V‡	141.15 cm^3·mol^{-1}
C_P	a†	641.5 J·K^{-1}·mol^{-1}
	b†	-7.87×10^{-3} J·K^{-2}·mol^{-1}
	c†	-234.12×10^5 J·K·mol^{-1}

* This error reflects only the uncertainty in $G^0_{natroalunite}$ at 250 °C and does not include errors resulting from inaccuracy or imprecision in the estimated thermodynamic parameters.

† Heat-capacity coefficients estimated by using data and techniques of Helgeson et al. (1978).

‡ Molar volume computed by using unit-cell data on natroalunite from Parker (1962).

We then computed $\Delta G^0_{f,natroalunite}$ at 25 °C and 1 bar by using the experimental value at 250 °C and estimates of the entropy and heat capacity of natroalunite obtained with the method of Helgeson et al. (1978). This method uses the entropies, molar volumes, and heat capacities of alunite, Na_2O, and K_2O to estimate entropy and heat capacity for natroalunite. These estimates are listed in Table 4.

Our computed $\Delta G^0_{f,natroalunite}$ at 25 °C and 1 bar is -4622.40 (± 1.91) kJ·mol^{-1}, where the error reflects only the uncertainty in ln $K_{(1)}$ at 250 °C and does not include possible inaccuracies or imprecision in the estimated thermodynamic properties for natroalunite or in the thermodynamic data on alunite, Na^+, or K^+ from Helgeson et al. (1978). Probably the greatest uncertainty involved in the calculation is in the free energy of formation of alunite at 25 °C. Published values range from -4672.27 kJ·mol^{-1} (Kashkai, 1975) to -4647.00 kJ·mol^{-1}, calculated using the free energy of formation of alunite at 90 °C from Ghiorso and Carmichael (1980) and the heat capacity of alunite from Kelley (1960). The -4659.30 kJ·mol^{-1} value from Helgeson et al. (1978) is roughly midway between these extremes.

Given this large uncertainty, our estimate of $\Delta G^0_{f,natroalunite}$ at 25 °C is in surprisingly good agreement with the -4622.35 kJ·mol^{-1} value reported by Hladky and Slansky (1981), the only published value for $\Delta G^0_{f,natroalunite}$ at 25 °C and 1 bar of which we are aware. Hladky and Slansky did not describe the estimation technique they used to obtain their value, and it is therefore difficult to assess its reliability. Moreover, their estimated log K of -5.14 for Reaction 1 at 25 °C is in poor agreement with our computed value of -2.83. We therefore conclude that the excellent agreement between the two estimates for $\Delta G^0_{f,natroalunite}$ at 25 °C is fortuitous.

We have also used the estimated thermodynamic properties of natroalunite to compute values for ln $K_{(1)}$ of -1.90 at 350 °C and 500 bars and -1.61 at 450 °C and 1000 bars. The estimated value at 350 °C is 0.17 log units more negative than the experimental value of -1.73. This is

within the estimated uncertainty of 0.26 for the experimentally determined value. At 450 °C, the estimated value is 0.62 log units more negative than the experimental value and far outside of its uncertainty of 0.05. There are several possible explanations for these discrepancies, including errors in the estimated entropy and heat capacity of natroalunite, or possibly some inaccuracies in the thermodynamic data from Helgeson et al. (1978). However, we feel that the most likely source of error is our assumption that the activity coefficients for Na^+ and K^+ cancel at 350 and 450 °C. The discrepancy between the estimated and experimentally determined values of ln $K_{(1)}$ is consistent with an increase in the value of ln γ_{Na^+} − ln γ_{K^+} at higher temperature, possibly caused by the observed increase in sulfuric acid concentration with temperature in the run product solutions.

Chemistry of natural alunites

We have examined the literature on alunite occurrences in an effort to find evidence for our predicted asymmetric solvus between alunite and natroalunite. Although compositional data are available on alunite from a variety of geologic environments, nearly all published analyses are of bulk samples. These do not provide information about small-scale compositional variations that might result from alunite-natroalunite exsolution. However, they do provide general information about the range of Na/K ratios in alunites from different settings.

Figure 8 presents published data on the Na content of natural alunites and natroalunites. We have subdivided these alunites into inferred high-, intermediate-, and low-temperature associations on the basis of their geologic setting and the associated minerals reported. Figure 8A includes compositional data on alunite associated with pyrophyllite in aluminous metamorphic rocks. These samples, which we interpret as the highest-temperature occurrence of natural alunite, are all high in Na, consistent with our experimental observation that increasing temperature favors more Na-rich alunites.

Figure 8B includes data on alunites from epithermal ore deposits and hot springs and spans a range of inferred temperatures from roughly 250 to 50 °C. Most of these data are from the Mount Lassen and Yellowstone geothermal areas (Ghiorso, 1980), the Summitville, Colorado, gold-quartz-alunite deposit (Stoffregen and Alpers, 1987; Stoffregen, unpublished data), and the Marysvale, Utah, alunite deposit (Schrader, 1913; Parker, 1962; Cunningham et al., 1984). Although Figure 8B does not provide good evidence for a solvus, we note that there are relatively few values near our predicted consolute composition of 64.5 mol% natroalunite.

Figure 8C includes data on alunites formed during weathering or diagenesis and shows a complete range of compositions. Although not considered in Figure 8C, these low-temperature alunites may also contain significant hydronium on the alkali site (Ross et al., 1968; Stoffregen and Alpers, in preparation). We do not feel that the observed range in Na contents indicates complete miscibility between alunite and natroalunite at near-surface conditions; instead, we attribute it to a lack of equilibration under these conditions. Disequilibrium between alunite and solution is also suggested by the work of Zotov (1971) and Ghiorso (1980) on hot-spring alunites. By assuming equilibrium between alunite and solution, both authors concluded that increasing temperature caused a decrease in the ln K of Reaction 1, a result inconsistent with our experiments. We suggest that chemical equilibrium is not generally attained between alunite and aqueous solutions below 100 °C.

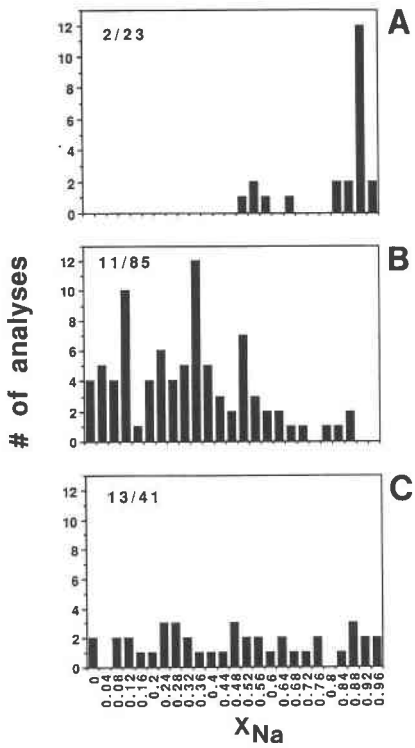

Fig. 8. Compositional data on natural alunites. Values in the left corner of the each figure give the number of localities represented followed by the total number of analyses shown. (**A**) Compositional data on alunite associated with pyrophyllite in aluminous metamorphic rocks from Wise (1975) and Schoch et al. (1985, 1989). (**B**) Compositional data on alunite from hydrothermal ore deposits (Schrader, 1913; Parker, 1962; Sheridan and Royse, 1970; Stoffregen and Alpers, 1987; Stoffregen, unpublished data;) and hot springs (Rusinov, 1966; Zotov, 1971; Slansky, 1975; Ghiorso, 1980). (**C**) Compositional data on alunite formed during diagenesis or weathering (Wherry, 1916; King, 1953; Moss, 1958; Keller et al., 1967; Ross et al., 1968; Goldbery, 1980; W. X. Chavez, personal communication, 1986; Chitale and Guven, 1987; Khoury, 1987; Rouchy and Pierre, 1987).

Although this lack of equilibration probably obscures any immiscibility between alunite and natroalunite in most low-temperature settings, there are some reports of coexisting alunite and natroalunite. Slansky (1975) described the occurrence of alunite and natroalunite from a "boiling pool" on White Island, New Zealand, and Aoki

(1983) identified alternating bands of alunite and natroalunite forming in the Osorezan geothermal field in Japan. Huang and Chang (1982) argued for an alunite-natroalunite solvus on the basis of equivocal compositional data from the Chinkuashih, Taiwan, gold-quartz-alunite deposit. Finally, we note that Parker (1962) was unable to synthesize alunite in the range Na_{40} to nearly Na_{100} at 100 °C, a result consistent with our inferred asymmetric solvus.

Conclusions

Our experimental study of alkali exchange between alunite and sulfate solutions has demonstrated that (1) the equilibrium constant for the reaction

$$KAl_3(SO_4)_2(OH)_6 + Na^+ = NaAl_3(SO_4)_2(OH)_6 + K^+$$

decreases with decreasing temperature; (2) alunite and natroalunite are completely miscible down to at least 350 °C; and (3) alunite and natroalunite form an asymmetric solid solution below 450 °C. Rigorous interpretation of the experimental results is hampered by a lack of equilibration at low temperature and by an inability to calculate activity coefficients in the aqueous phase at higher temperatures. Evaluation of mixing relations in the aqueous phase is also complicated by the generation of sulfuric acid during our 350 and 450 °C experiments. This acid production may have increased the experimental K_D values, causing us to overestimate ln $K_{(1)}$ for the alkali-exchange reaction at these temperatures.

We have fit our experimental data by using a subregular Margules model for alunite-natroalunite mixing. Uncertainties in the Margules parameters increase substantially with decreasing temperature because of a decrease in the quality of the experimental reversals with decreasing temperature and the limited range of solid compositions used at 250 °C. Nevertheless, the subregular Margules model used in this study is superior to other assumptions, such as ideal mixing, that are contradicted by our experiments. In addition, the estimated Margules parameters provide a basis for interpreting the chemistry of alunites formed at or above 250 °C. Detailed study of the chemistry of natural alunites and coexisting aqueous solutions may help to refine our proposed mixing terms and may also confirm the existence of an asymmetric solvus in the alunite-natroalunite system. This solvus is suggested but not required by our experimental results.

Acknowledgments

We thank J. J. Hemley and M. J. Holdaway for use of experimental facilities at the U.S. Geological Survey, Reston, Virginia, and Southern Methodist University, Dallas, Texas, respectively. Helpful reviews of this paper were provided by J. J. Hemley and M. J. Holdaway and also by Charlie Alpers, Phil Candela, Rob Robinson, Bruce Hemingway, and Paul Barton. We also thank G. J. Buekes and W. X. Chavez for providing unpublished data on alunites from several localities. This work was supported in part by the USGS and by the Institute for the Study of Earth and Man, Southern Methodist University.

References cited

Altaner, S.P., Fitzpatrick, J.J., Krohn, M.D., Bethke, P.M., Hayba, D.O., Goss, J.A., and Brown, Z.A. (1988) Ammonium in alunites. American Mineralogist, 73, 145–152.

Ames, L.I., Jr. (1964) Some zeolite equilibria with alkali metal cations. American Mineralogist, 49, 127–145.

Aoki, M. (1983) Modes of occurrence and mineralogical properties of alunite solid solution in Osorezan geothermal area. Science Reports, Hirosake University, 30, 132–141 (in Japanese).

Botinelly, T. (1976) A review of the minerals of the alunite-jarosite, beudantite, and plumbogummite groups. Journal of Research of the U.S. Geological Survey, 4, 213–216.

Brimhall, G.H., Jr. (1980) Deep hypogene oxidation of porphyry copper potassium-silicate protore at Butte, Montana: A theoretical evaluation of the copper remobilization hypothesis. Economic Geology, 75, 384–409.

Chanh, N.B. (1964) Equilibres des systèms binaires d'halogenures de sodium et potassium à l'état solide. Journal de Chimie Physique, 61, 1428–1433.

Chatterjee, N.D., and Flux, S. (1986) Thermodynamic mixing properties of muscovite-paragonite crystalline solutions at high temperatures and pressures, and their geological applications. Journal of Petrology, 27, 677–693.

Chitale, D.V., and Guven, N. (1987) Natroalunite in a laterite profile over Deccan Trap basalts at Matanumad, Kutch, India. Clays and Clay Minerals, 35, 196–202.

Cunningham, C.G., Rye, R.O., Steven, T.A., and Mehnert, H.H. (1984) Origins and exploration significance of replacement and vein-type alunite deposits in the Marysvale volcanic field, west central Utah. Economic Geology, 79, 38–50.

Davey, P.T., Lukaszewski, G.M., and Scott, T.R. (1963) Thermal decomposition of the basic aluminium sulphate, $3Al_2O_3 \cdot 4SO_3 \cdot 9H_2O$. Australian Journal of Applied Science, 14, 137–154.

Davies, P.K., and Navrotsky, A. (1983) Quantitative correlations of deviations from ideality in binary and pseudobinary solid solutions. Journal of Solid State Chemistry, 46, 1–22.

Fielding, J.F. (1980) Crystal chemistry of the oxonium alunite–potassium alunite series, 121 p. M.S. thesis, Lehigh University, Bethlehem, Pennsylvania.

Ghiorso, M.S. (1980) Mineral-solution equilibria in volcanic hot springs, 381 p. Ph.D. thesis, University of California, Berkeley, California.

Ghiorso, M.S., and Carmichael, I.E. (1980) Solubility studies on the minerals alunite and kaolinite: Free energy of formation of alunite and data on the kinetics of dissolution of kaolinite at 90 °C and 1 bar. Geological Society of America Abstracts with Programs, 12, 433.

Goldbery, R. (1980) Early diagenetic, Na-alunites in Miocene algal mat intertidal facies, Ras Sudar, Sinai. Sedimentology, 27, 189–198.

Green, E.J. (1970), Predictive thermodynamic models for mineral systems. I. Quasi-chemical analysis of the halite-sylvite subsolidus. American Mineralogist, 55, 1692–1713.

Guggenheim, E.A. (1952) Mixtures. Clarendon Press, Oxford, England.

Harvie, C.E., Moeller-Weare, N., and Weare, J.H. (1984) The prediction of mineral solubility in natural waters: The Na-K-Mg-Ca-Cl-H-SO_4-OH-HCO_3-CO_3-CO_2-H_2O system to high ionic strengths at 25 °C. Geochimica et Cosmochimica Acta, 48, 723–751.

Helgeson, H.C., and Kirkham, D.H. (1974) Theoretical prediction of the thermodynamic behavior of aqueous electrolytes at high pressures and temperatures. I. Summary of the thermodynamic/electrostatic properties of the solvent. American Journal of Science, 274, 1089–1198.

Helgeson, H.C., Delany, J.M., Nesbitt, H.W., and Bird, D.K. (1978) Summary and critique of the thermodynamic properties of rock-forming minerals. American Journal of Science, 278-A, 1–229.

Hemley, J.J., Hostetler, P.B., Gude, A.J., and Mountjoy, W.T. (1969) Some stability relations of alunite. Economic Geology, 64, 599–612.

Hladky, G., and Slansky, E. (1981) Stability of alunite minerals in aqueous solutions at normal temperature and pressure. Bulletin de Minéralogie, 104, 468–477.

Holmes, H.F., and Mesmer, R.E. (1986) Thermodynamics of aqueous

solutions of alkali metal sulfates. Journal of Solution Chemistry, 15, 495–518.
Huang, C.K., and Chang, Y.H. (1982) Barite and alunite from the Chinkuashih gold-copper deposits, Taiwan. Acta Geologica Taiwanica, 21, 1–13.
Kashkai, Ch.M. (1975) Determination of $\Delta G^0_{f,298}$ of synthetic jarosite and its sulfate analogues. Geokhimyia, 5, 778–784 (in Russian).
Keller, W.D., Gentile, R.J., and Reesman, A.L. (1967) Allophane and Na-rich alunite from kaolinitic nodules in shale. Journal of Sedimentary Petrology, 37, 215–220.
Kelley, K.K. (1960) Contributions to the data on theoretical metallurgy. XIII. High temperature heat content, heat capacity and entropy data for the elements and inorganic compounds. U.S. Bureau of Mines Bulletin 584, 232 p.
Khoury, H.N. (1987) Alunite from Jordan. Neues Jahrbuch für Mineralogie, Monatshefte, 426–432.
King, D. (1953) Origin of alunite deposits at Pidinga, South Australia. Economic Geology, 48, 689–703.
Meyer, C., and Hemley, J.J. (1967) Wall rock alteration. In H.L. Barnes, Ed., Geochemistry of hydrothermal ore deposits, p. 166–235. Holt, Rhinehart, and Winston, New York,
Moss, A.A. (1958) Alumian and natroalunite. Mineralogical Magazine, 31, 884–885.
Ossaka, J., Hirabayashi, J.-I., Okada, K., and Kobayashi, R. (1982) Crystal structure of minamiite, a new mineral of the alunite group. American Mineralogist, 67, 114–119.
Pabalan, R.T., and Pitzer, K.S. (1987) Thermodynamics of concentrated electrolyte mixtures and the prediction of mineral solubilities to high temperatures for mixtures in the system Na-K-Mg-Cl-SO_4-OH-H_2O. Geochimica et Cosmochimica Acta, 51, 2429–2444.
Parker, R.L. (1962) Isomorphous substitution in natural and synthetic alunite. American Mineralogist, 47, 127–136.
Pascal, M.L., and Roux, J. (1985) K-Na exchange equilibria between muscovite-paragonite solid solution and hydrothermal chloride solutions. Mineralogical Magazine, 49, 515–521.
Perrier, C., and Bellanca, A. (1940) Periodico Mineral., 11,169 (extracted from M. K. Reser, Ed., Phase diagrams for ceramists, 1969 Supplement, p. 252. The American Ceramic Society, Columbus, Ohio).
Pitzer, K.S., Roy, R.N., and Silvester, L.F. (1977) Thermodynamics of electrolytes: 7. Sulfuric acid. Journal of the American Chemical Society, 99, 4930–4936.
Pitzer, K.S., Peiper, J.C., and Busey, R.H. (1984) Thermodynamic properties of aqueous sodium chloride solutions. Journal of Physical and Chemical Reference Data, 13, 1–102.
Powell, R. (1974) A comparison of some mixing models for crystalline silicate solutions. Contributions to Mineralogy and Petrology, 46, 265–274.
——— (1987) Darken's quadratic formalism and the thermodynamics of minerals. American Mineralogist, 72, 1–12.
Raymahashay, B.C. (1969) A geochemical study of rock alteration by hot springs in the Paint Pot Hill area, Yellowstone Park. Geochimica et Cosmochimica Acta, 32, 499–522.
Ripmeester, J.A., Ratcliffe, C.I., Dutrizac, J.E., and Jambor, J.L. (1986) Hydronium ion in the alunite-jarosite group. Canadian Mineralogist, 24, 435–447.
Ross, C.S., Harlan, R.B., Monroe, W.H., Fahey, J.J., and Ross, M. (1968) Natroalunite in Upper Cretaceous sedimentary rocks, north-central Texas. Journal of Sedimentary Petrology, 38, 1155–1165.
Rouchy, J.M., and Pierre, C. (1987) Authigenic natroalunite in middle Miocene evaporites from the Gulf of Suez (Gemas, Egypt). Sedimentology, 34, 807–812.
Rusinov, V.D. (1966) Alunitization processes in some regions of young volcanism. In Metasomaticheskie izmeneniya bokovikh pored i ikh rol v rudoodrazzovanii. Nedra, Moscow (in Russian).
Schoch, A.E., Beukes, G.J., and Praekelt, H.E. (1985) A natroalunite-zaherite-hotsonite paragenesis from Pofadder, Bushmanland, South Africa. Canadian Mineralogist, 23, 29–34.
Schoch, A.E., Beukes, G.J., van der Westhuizen, W.A., and de Bruiyn, H. (1989) Natroalunite from Koenabib, Pofadder district, South Africa. South African Journal of Geology (Suid-Afrikaanse Tydskrif vir geologie), 92, 20–28.
Schoen, R., White, D.E., and Hemley, J.J. (1974) Argillization by descending acid at Steamboat Springs, Nevada. Clays and Clay Minerals, 22, 1–22.
Schrader, F.C. (1913) Alunite in Patagonia, Arizona, and Bovard, Nevada. Economic Geology, 8, 752–767.
Scott, K.M. (1987) Solid solution in, and classification of, gossan-derived members of the alunite-jarosite family, northwest Queensland, Australia. American Mineralogist, 72, 178–187.
Shannon, R.D. (1976) Revised effective ionic radii and systematic studies of interatomic distances in halides and chalcogenides. Acta Crystallographica, A32, 751–767.
Sheridan, M.F., and Royse, C.F., Jr. (1970) Alunite: A new occurrence near Wickenburg, Arizona. American Mineralogist, 55, 2016–2022.
Slansky, E. (1975) Natroalunite and alunite from White Island Volcano, Bay of Plenty, New Zealand. New Zealand Journal of Geology and Geophysics, 18, 285–293.
Stoffregen, R.E., and Alpers, C.N. (1987) Woodhouseite and svanbergite in hydrothermal ore deposits: Products of apatite destruction during advanced argillic alteration. Canadian Mineraologist, 25, 201–211.
Thompson, J.B., Jr., and Waldbaum, D.R. (1968) Mixing properties of sanidine crystalline solutions: I. Calculations based on ion-exchange data. American Mineralogist, 53, 1965–1999.
——— (1969) Mixing properties of sanidine crystalline solutions: III. Calculations based on two-phase data. American Mineralogist, 54, 811–838.
Wherry, E.T. (1916) Notes on alunite, psilomelanite, and titanite. United States National Museum Proceedings, 51, 81–88.
Wise, W.S. (1975) Solid solution between the alunite, woodhouseite, and crandallite mineral series. Neues Jahrbuch für Mineralogie, Monatschafte, 540–545.
Zen, E-an. (1972) Gibbs free energy, enthalpy, and entropy of ten rock-forming minerals: Calculations, discrepancies, implication. American Mineralogist, 57, 524–553.
Zotov, A.V. (1971) Dependence of the composition of alunite on the temperature of its formation. Geokhimiya, 110–113.

Manuscript received April 10, 1989
Manuscript accepted September 29, 1989

Appendix 1. Calculation of activity coefficients at 250 °C

We have used Pitzer's equations to compute individual-ion activity coefficients for Na^+ and K^+ at 250 °C and 500 bars. In making these calculations, we assumed that the equation giving the temperature dependence of $B^{(0)}$, $B^{(1)}$, and $C^{(\phi)}$ from 25 to 225 °C (Holmes and Mesmer, 1986) could be extrapolated to 250 °C, and we neglected the effects of changes in pressure. Following Pabalan and Pitzer (1987), we set $\theta_{Na,K}$ equal to its 25 °C value of −0.012. Similarly, because no data is available on $\psi_{Na\text{-}K\text{-}SO_4}$ at elevated temperature, we used the 25 °C value of −0.010. The Debye-Hückel A term at 250 °C and 500 bars was interpolated from values tabulated by Pitzer et al. (1984) as 0.68. As recommended by Holmes and Mesmer, α was set to 1.4. Pitzer coefficients for sulfuric acid and dissolved Al are not now available at 250 °C, and as a result we have neglected these species in the calculations. Because of their low concentrations compared to the amount of dissolved sodium and potassium sulfate,

TABLE A1. Calculated individual-ion activity coefficients at 250 °C and 500 bars

Run	N_{Na}	γ_{Na^+}	γ_{K^+}	$\ln \gamma_{Na^+} - \ln \gamma_{K^+}$
13	0.904	0.471	0.461	0.021
42	0.911	0.471	0.461	0.021
43	0.590	0.467	0.466	0.003
85	0.701	0.469	0.464	0.010
86	0.850	0.470	0.462	0.018
87	0.934	0.471	0.460	0.023
88	0.967	0.472	0.460	0.025

they are unlikely to have a significant effect on the computed values of γ_{Na^+} and γ_{K^+}.

Computed values of Na^+ and K^+ individual-ion activity coefficients are tabulated in Table A1 for all runs at 250 °C, along with the quantity $\ln \gamma_{Na^+} - \ln \gamma_{K^+}$. Note that this quantity is always less than 0.03. This represents a negligible amount compared to the measured range of $\ln K_D$ at this temperature (Table 1 and Fig. 3C) and has been ignored in the calculation of $\ln K_{(1)}$ and the alunite-natroalunite mixing parameters.